

Use of artificial intelligence techniques to predict distribution of heavy metals in groundwater of Lakan lead-zinc mine in Iran

Z. Bayatzadeh Fard, F. Ghadimi* and H. Fattahi

Department of Mining Engineering, Arak University of Technology, Arak, Iran

Received 10 January 2016; received in revised form 6 February 2016; accepted 22 February 2016

*Corresponding author: ghadimi@arakut.ac.ir (F. Ghadimi).

Abstract

Determining the distribution of heavy metals in groundwater is important in developing appropriate management strategies at mine sites. In this paper, the application of artificial intelligence (AI) methods to data analysis, namely artificial neural network (ANN), hybrid ANN with biogeography-based optimization (ANN-BBO), and multi-output adaptive neural fuzzy inference system (MANFIS) to estimate the distribution of heavy metals in groundwater of Lakan lead-zinc mine is demonstrated. For this purpose, the contamination groundwater resources were determined using the existing groundwater quality monitoring data, and several models were trained and tested using the collected data to determine the optimum model that used three inputs and four outputs. A comparison between the predicted and measured data indicated that the MANFIS model had the most potential to estimate the distribution of heavy metals in groundwater with a high degree of accuracy and robustness.

Keywords: *Groundwater, ANN, MANFIS, Heavy Metals, Biogeography-Based Optimization Algorithm.*

1. Introduction

Mining and mine-related industries have the potential significant environmental impacts due to the formation of acid drainage, and the release of toxic compounds such as heavy metals into groundwater. Acid mine drainage (AMD) generated through the oxidation of sulfide minerals such as pyrite, marcasite, and jarosite is characterized by high concentrations of iron, dissolved sulfate, low pH, and variable concentrations of metals and rare earth elements (REEs) [1]. In particular, toxic metals such as Pb, Zn, Cu, Mn, and Cd are released into the environment under the condition of low pH, which can be harmful to the living organisms. The common methods used for measuring heavy metals in AMD are time-consuming and may be prohibitively-expensive in countries with limited resources. Therefore, other tools are required to determine the distribution of groundwater contamination at mine sites that use analytes that can be sampled and analyzed more cheaply, and that can be used as proxies for the distribution of

metals in groundwater. Artificial intelligence (AI) techniques are among the most used to assess the groundwater quality data. The algorithms and methods studied in AI include knowledge-based systems (KBSs), genetic algorithms (GAs), biogeography-based optimization (BBO), artificial neural networks (ANNs), fuzzy logic (FL), and adaptive neural fuzzy inference system (ANFIS). Recent investigations have highlighted the application of the AI techniques to the environmental engineering problems. ANNs have obtained an increasing recognition in different environmental engineering fields in the past few decades because of their ability to extract complex and non-linear relationships from datasets. Rogers and Dowla (1994) began to optimize groundwater remediation using an ANN with a parallel solute transport modeling [2]. Schleiter et al. (1999) modeled water quality, bio-indication, and population dynamics in ecosystems using ANN [3]. Cigizoglu (2002) estimated the suspended sediment for rivers using ANN and sediment

rating curves [4]. Kemper and Sommer (2002) anticipated the heavy metal concentration in soils from reflectance spectroscopy using back-propagation neural network (BPNN) and multiple linear regression (MLR) [5]. Liu et al. (2004) evaluated the ability of a BPNN model to forecast the variation in the groundwater quality of an area in Taiwan [6]. Almasri and Kaluarachchi (2005) used the modular neural networks to forecast the nitrate distribution in groundwater using the on-ground nitrogen-loading and recharge data [7]. Palani et al. (2008) used ANN to predict and forecast the quantitative characteristics of Singapore coastal water bodies [8]. Noori et al. (2010) used ANN and principal component analysis-MLR models in order to forecast the river flow based on the developed discrepancy ratio statistic [9]. Rooki et al. (2011) predicted heavy metals in AMD using BPNN, general regression neural network (GRNN), and MLR in the Shur River of the Sarcheshmeh porphyry copper mine, SE of Iran [10]. Heydari et al. (2013) developed the ANN models to calculate the monthly values of dissolved oxygen and specific conductance as two water quality parameters of Delaware River at a station situated at Pennsylvania site in the US [11]. Badaoui et al. (2013) applied an ANN of MLP type for the anticipation of the levels of heavy metals in Moroccan aquatic sediments [12]. Irfan Yesilnacar and Sahinkaya (2012) applied ANN for prediction of sulfate and SAR in an unconfined aquifer in Turkey [13]. Keskin et al. (2015) used ANN for the prediction of water pollution sources in Turkey [14]. Nasr and Zahran (2014) used pH as a tool to predict salinity of groundwater for the irrigation purpose using ANNs [15]. Grande et al. (2009) applied a fuzzy logic qualitative model to the presence of As in the fluvial network due to the AMD processes in the RioTinto mining area (SW Spain) [16]. Yan et al. (2010) developed ANFIS for the classification of water quality status [17]. Sahu et al. (2010) used fuzzy logic and ANN models to predict the spontaneous heating susceptibility of Indian coals [18]. Valente et al. (2013) used the fuzzy inference system to estimate the concentration of metals in AMD [19]. Mohammadi and Meech (2012) applied the AFRA-heuristic expert system to assess the atmospheric risk of sulfide waste dumps [20]. Zhang et al. (2012) used fuzzy cognitive maps and policy option simulations analysis for a coalmine ecosystem in China [21]. Liu and Zou (2012) used improved fuzzy matter-element method to evaluate water quality in China

[22]. Pourjabbar et al. (2014) used fuzzy divisive hierarchical clustering (FDHC) and fuzzy hierarchical cross-clustering (FHCC) to investigate the source of contamination near an abandoned uranium mine in Germany [23]. Mahdevari et al. (2014) used the fuzzy TOPSIS model to assess the human health and safety risks in underground coal mines [24]. Chang et al. (2014) used the neuro-fuzzy networks with factor analysis to assess arsenic concentration in Huang gang Creek in northern Taiwan [25]. Maiti and Tiwari (2014) applied artificial neural networks, Bayesian neural networks, and adaptive neuro-fuzzy inference system for the prediction of groundwater level [26]. Ghadimi (2015) predicted heavy metals (Pb, Zn, and Cu) in the groundwater from Arak city using the ANN algorithm by taking major elements (HCO_3 , SO_4) in the groundwater from Arak city [27].

This paper focuses on predicting the distribution of heavy metals in groundwater resources impacted by Lakan lead-zinc processing plant near the city of Khomein, central Iran. The objectives of this study were as follows: 1) to explore applications of the MANFIS, ANN, and ANN-BBO methods in predicting heavy metals in AMD 2) to develop a model based on MANFIS, and evaluate the applicability of the ANFIS approach to assess and predict heavy metals in AMD, and compare the performance with ANN 3) to provide useful information regarding the environmental management of lead and zinc processing plants.

2. Hydrogeological setting and sampling

The Lakan mining area is located near the city of Khomein, central Iran. A tailings dam, a lead-zinc processing plant, and a lead-zinc mine are located 40 km from Khomein city. The region is underlain by the crystalline limestone of Cretaceous period and the low-grade metamorphic rocks (Figure 1) in Sannandaj-Sirjan metamorphic belt [28]. A shallow aquifer was developed into the Quaternary sediments, which are underlain by limestone bedrock. The mining activities in the region commenced in 1990. During the operational period of the mine, mining wastes were discharged from the mine to a tailings site 200 meters downstream from the mine and directly to a river. The oxidation of sulfide minerals in mine wastes has caused metals and other chemical constituents to be leached to groundwater. Groundwater was thus exposed to severe heavy metal pollution from the tailings materials and other mine wastes.

52 groundwater samples were collected from around the Lakan mining area in February 2008 (some are shown in Figure 1). Hydro-chemical parameters of water samples including Fe, Mn,

Pb, Zn, Hg, Cl, SO₄ ions, cyanide, and TDS were measured by inductively-coupled plasma mass spectrometer (ICP-MS) in the uranium conversion facility (UCF) Company [29].

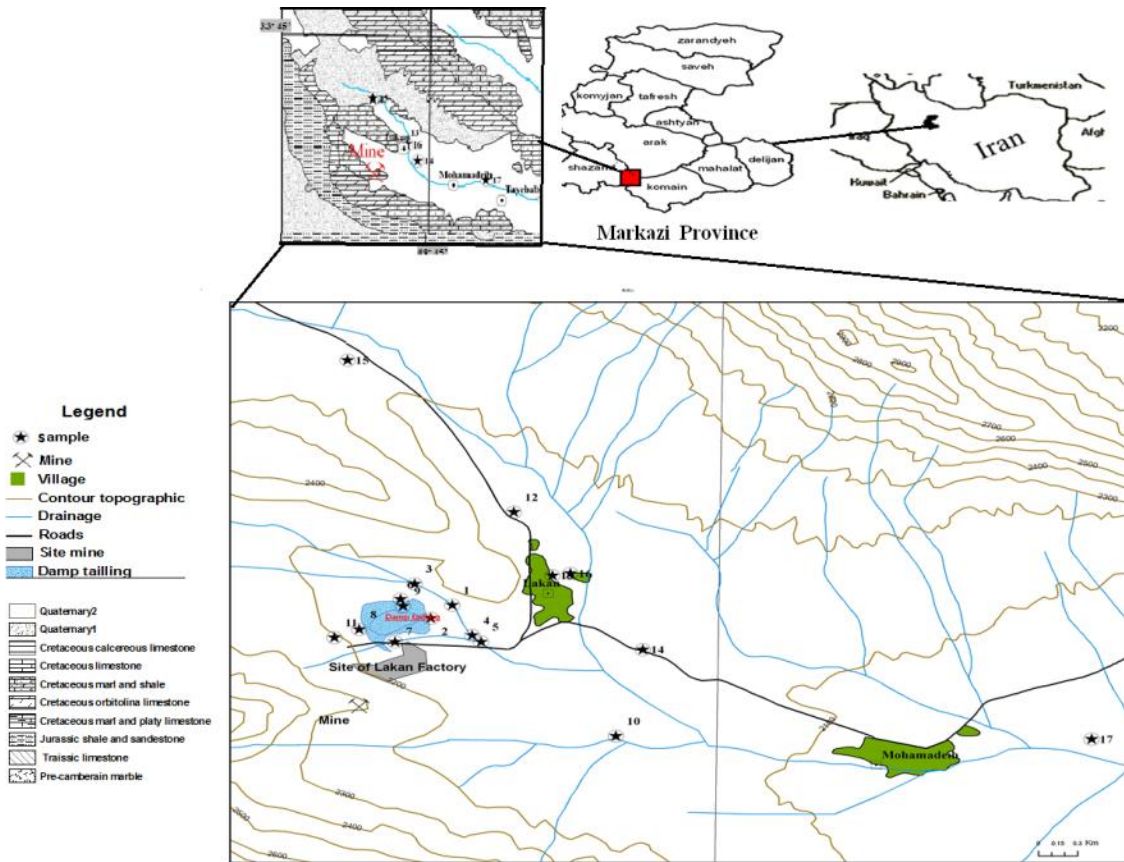


Figure 1. Geological map of the desired area.

3. Data analysis

In order to analyze the data, different modeling methods were employed in this study. The following sections describe implementation of the aforementioned methods to predict the distribution of heavy metals in groundwater. Subsequently, concentrations of the heavy metals obtained in the laboratory were compared with their corresponding predicted concentrations. Descriptive statistics of the data are shown in Table 1.

Table 1. Descriptive statistics of data.

Variab les	Vali d N	Mea n	Minimu m	Maximu m	Standar d deviatio n
SO4	52	167	15	338	126
Cl	52	4.27	0.01	13	3.74
TDS	52	243	31	473	156
Fe	52	0.16	0.01	0.68	0.19
Mn	52	0.17	0.01	0.53	0.17
Pb	52	0.08	0.01	0.22	0.06
Zn	52	0.72	0.01	2.79	0.92

For the purpose of calculation and modeling, a correlation matrix was created (). Using this table, the parameters SO₄, Cl, and TDS were selected to be the model inputs due to their strong correlations with the heavy metal (Fe, Mn, Pb, and Zn) concentrations. The model outputs were concentrations of the heavy metals including Fe, Mn, Pb, and Zn. In this study, normalization of the data (inputs and outputs) was carried out in the range of (0, 1) using Eq. 1, and the number of training data (38) and test data (14) were then selected randomly.

$$P_n = \frac{P - P_{\min}}{P_{\max} - P_{\min}} \quad (1)$$

where P_n is the normalized parameter, p denotes the actual parameter, P_{\min} represents a minimum of the actual parameters, and P_{\max} stands for a maximum of the actual parameters. Two criteria were used to evaluate the effectiveness of each

model and its ability to make accurate predictions. The mean square error (MSE) can be calculated as follows (Eq. 2):

$$MSE = \frac{1}{n} \sum_{i=1}^n (y_i - y'_i)^2 \tag{2}$$

Where y_i is the measured value, y'_i denotes the predicted value, and n stands for the number of samples. MSE indicates the discrepancy between the measured and predicted values. The lower the MSE, the more accurate the prediction is.

Furthermore, the efficiency criterion, R^2 , is given by Eq. 3:

$$R^2 = 1 - \frac{\sum_{i=1}^n (y_i - y'_i)^2}{\sum_{i=1}^n y_i^2 - \frac{\sum_{i=1}^n y_i'^2}{n}} \tag{3}$$

where R^2 efficiency criterion represents the percentage of the initial uncertainty explained by the model. The best fitting between the measured and predicted values, which is unlikely to occur, would have $MSE = 0$ and $R^2 = 1$.

Table 1. Descriptive statistics of data.

Variables	Valid N	Mean	Minimum	Maximum	Standard deviation
SO ₄	52	167	15	338	126
Cl	52	4.27	0.01	13	3.74
TDS	52	243	31	473	156
Fe	52	0.16	0.01	0.68	0.19
Mn	52	0.17	0.01	0.53	0.17
Pb	52	0.08	0.01	0.22	0.06
Zn	52	0.72	0.01	2.79	0.92

Table 2. Correlation matrix between heavy metal concentrations and independent variables.

	SO ₄	Cl	TDS	Fe	Mn	Pb	Zn	Hg	CN
SO ₄	1								
Cl	0.892	1							
TDS	0.919	0.890	1						
Fe	-0.492	-0.560	-0.644	1					
Mn	0.579	0.461	0.640	-0.339	1				
Pb	0.628	0.628	0.536	-0.125	0.322	1			
Zn	0.701	0.568	0.774	-0.375	0.608	0.250	1		
Hg	-0.178	-0.093	-0.048	-0.118	-0.180	-0.177	-0.137	1	
CN	-0.166	-0.093	-0.068	-0.076	-0.142	-0.162	-0.118	0.287	1

4. A brief review of methods used in this study

4.1. Artificial neural networks (ANNs)

Since 1940s, ANNs have been used in many applications in engineering and science [30]. The principles of ANNs are based upon the human brain operations. Actually, ANNs try to imitate the way that human brain solves the problems or remembers things. ANNs have different structures including at least two layers (input and output layers). Between these two layers, there can be one or more layers called hidden layers. Each layer consists of several neurons depending on the position of the layer. The number of neurons in the input layer represents the number of parameters used for prediction, and the number of neurons in the output layer represents the number of variables to be predicted. The neurons in the hidden layers are arranged arbitrarily. The neurons of a layer are joined to the neighbor layer

neurons by connections called weights. Pairs of inputs and outputs are fed to the ANN, and the network creates the initial weights randomly. The objective is to find the value of the weight that minimizes the differences between the actual output and the predicted output in the output layer in order to minimize the mean square errors (MSEs), the average squared error between the network predicted outputs and the target output [31]. This process is called learning in the ANN. There are large numbers of different algorithms adjusting the weights.

Multilayer perceptron is a feed-forward neural network, where signals always travel in the direction of the output layer. A typical multilayer perceptron with one hidden layer can be mathematically expressed as indicated in Eqs. 4-7.

The outputs of the hidden layer (Z_j) are obtained as (1) summing the products of the inputs (X_i) and weight vectors (a_{ij}) and a hidden layer bias term (a_{0j} ; see Eq. 4), and (2) transforming this sum using transfer function g (see Eq. 5). The most widely used transfer functions are logistic and hyperbolic tangents. Similarly, the outputs of the output layer (Y_k) are obtained by (1) summing the products of the hidden layer outputs (Z_j) and weight vectors (b_{jk}) and output layer bias term (b_{0k} ; see Eq. 6 and Figure 2), transforming this sum using transfer function g (see Eq. 7 and Figure 2).

$$u_j = \sum_{i=1}^{N_{inp}} x_i a_{ij} + a_{0j} \quad (4)$$

$$Z_j = g(u_j) \quad (5)$$

$$v_k = \sum_{j=1}^{N_{hid}} Z_j b_{jk} + b_{0k} \quad (6)$$

$$Y_k = g(v_k) \quad (7)$$

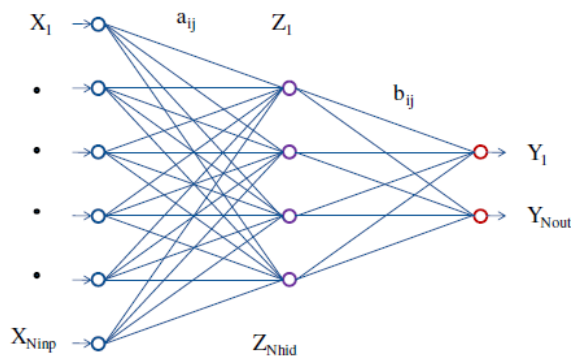


Figure 2. Multilayer perceptron neural networks.

4.2. Biogeography-based optimization (BBO)

Biogeography-based optimization (BBO) is an evolutionary algorithm that is inspired by biogeography [33]. In BBO, a biogeography habitat indicates a candidate optimization problem solution, and it is comprised of a set of features, which are also called decision variables or independent variables. A set of biogeography habitats denotes a population of candidate solutions, and the habitat suitability index (HSI) in biogeography denotes the fitness of a candidate solution. Like other evolutionary algorithms, each candidate solution in BBO probabilistically shares the decision variables with other candidate solutions to improve the candidate solution fitness. This sharing process is analogous to migration in biogeography, i.e. each candidate solution immigrates decision variables from other

candidate solutions based on its immigration rate, and emigrates decision variables to other candidate solutions based on its emigration rate. BBO consists of two main steps, migration and mutation. This algorithm can be used to optimize the ANN parameters. In this study, we used BBO to better regulate the weights and biases of the ANN model.

4.3. Adaptive neuro-fuzzy inference system (ANFIS)

The fuzzy logic system forms a system with the help of fuzzy rules [34]. ANFIS is a multilayer (five-layer) feed-forward network that uses neural network learning algorithms and fuzzy logic to map an input space to an output space. Each layer contains several nodes described by the node function. The adaptive nodes denoted by squares represent the parameter sets that are adjustable in these nodes and are changed in each of the learning iterations, whereas the fixed nodes, denoted by circles, represent the parameter sets that are fixed in the system. There are three types of ANFIS techniques, namely grid partitioning (GP), subtractive clustering method (SCM), and fuzzy C-means (FCM) techniques. The GP method generates a single-output Sugeno-type FIS on the data. The SC and FCM methods can be used for multi-output ANFIS. In these methods, depending on the types of inference operations upon “if-then rules”, they can be classified into two types, namely Mamdani’s system and Sugeno’s system. Mamdani’s system is the most commonly used one in various applications. Sugeno’s system is also more compact and computationally efficient than the Mamdani’s system [35].

For a first-order Sugeno fuzzy model, a typical rule set with two fuzzy if-then rules, can be expressed as follows:

$$\text{Rule 1: if } x \text{ is } A_1 \text{ } y \text{ is } B_1, \quad (8)$$

$$\text{then } f_1 = p_1^x + q_1^y + r_1$$

$$\text{Rule 2: if } x \text{ is } A_2 \text{ } y \text{ is } B_2, \quad (9)$$

$$\text{then } f_2 = p_2^x + q_2^y + r_2$$

where x and y are inputs, and f is output. A_1 , A_2 , B_1 , and B_2 are non-linear parameters, and p_1 , p_2 , q_1 , and q_2 are linear parameters. The outputs of each node in layer 1 are calculated as:

$$O_{1,i} = \mu_{A_i}(x) \quad \text{for } i=1,2 \quad (10)$$

$$O_{1,i} = \mu_{B_{i-z}}(y) \quad \text{for } i=3,4 \quad (11)$$

where $O_{1,i}$ is the output of the i^{th} node of first layer, and $\mu(x)$ and $\mu(y)$ represent the appropriate parameterized MFs. The adaptive nodes can adopt any fuzzy membership function (MF). It should be noted that a bell-shaped membership function is generally used as the input MF (Eq. 12):

$$O_{2,i} = \frac{1}{1 + \left(\frac{x - c_i}{a_i} \right)^{2b_i}} \quad (12)$$

where a_i and b_i change the width of the curve, and c_i indicates the center of the curve. In the second layer of ANFIS, which is labeled as sign ‘ Π ’, the outputs of the previous layer are multiplied by each other in the related node.

$$O_{2,i} = \mu_{A_i}(x) * \mu_{B_i}(y) \quad \text{for } i=1,2 \quad (13)$$

where $O_{2,i}$ is the output of the i^{th} node of the second layer. The number of nodes in layer 2 is dictated by fuzzy rules, and each node in the layer

is considered as a fixed node. The normalization of the pervious layer is described by the following equation:

$$O_{3,i} = \bar{w}_i = \frac{w_i}{w_1 + w_2} \quad \text{for } i=1,2 \quad (14)$$

Each node in the third layer is a fixed one, which is labeled as ‘Norm’. In layer 4, the outputs are calculated as follows:

$$O_{4,i} = \bar{w}_i f_i$$

All of the outputs of the 4th layer are added to the 5th layer with a single node, which is labeled as ‘Sum’. The node in the 5th layer computes the output of the whole network:

$$O_{5,i} = \sum_{i=1} \bar{w}_i f_i$$

However, in this study, we used the multi-output ANFIS (MANFIS), and so a simple example with one input one rule first-order Sugeno and three outputs for this method are listed below (Figure 3) [35].

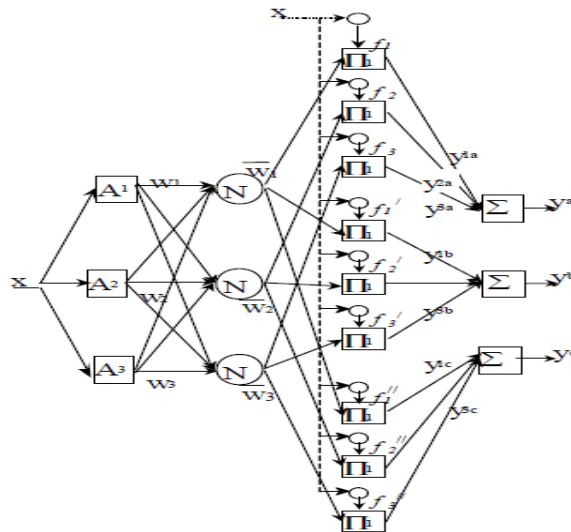


Figure 3. MANFIS architecture with three outputs [35].

Layer 1. Generate the membership grades:

$$o_i^1 = g(x) \quad (15)$$

where g is the membership function of the MANFIS system.

Layer 2. Generate the firing strengths:

$$o_i^2 = w_i = \prod_{j=1}^m g_j(x) \quad (16)$$

Layer 3. Normalize the firing strengths:

$$o_i^3 = \bar{w}_i = \frac{w_i}{w_1 + w_2 + w_3} \quad (17)$$

Layer 4. Calculate the rule outputs based on the consequent parameters:

$$o_i^4 = y_i = \bar{w}_i \cdot f_i = \bar{w}_i \cdot (p_i \cdot x + q_i \cdot x + r_i) \quad (18)$$

$$o_i^{4'} = y_i' = \bar{w}_i \cdot f_i' = \bar{w}_i \cdot (p_i' \cdot x + q_i' \cdot x + r_i') \quad (19)$$

$$o_i^{4''} = y_i'' = \bar{w}_i \cdot f_i'' = \bar{w}_i \cdot (p_i'' \cdot x + q_i'' \cdot x + r_i'') \quad (20)$$

Layer 5. Sum all the inputs from layer 4:

$$o_i^5 = y_a = \sum_{i=1}^n y_i = \sum_{i=1}^n \bar{w}_i \cdot f_i = \bar{w}_i \cdot (p_i \cdot x + q_i \cdot x + r_i) \quad (21)$$

$$o_i^{5'} = y_b = \sum_{i=1}^n y_i' = \sum_{i=1}^n \bar{w}_i \cdot f_i' = \bar{w}_i \cdot (p_i' \cdot x + q_i' \cdot x + r_i') \quad (22)$$

$$o_i^{5''} = y_c = \sum_{i=1}^n y_i'' = \sum_{i=1}^n \bar{w}_i \cdot f_i'' = \bar{w}_i \cdot (p_i'' \cdot x + q_i'' \cdot x + r_i'') \quad (23)$$

MANFIS for the three outputs comprises a lone input, thus there are no therefore rules of inference for this system, although there exists an operation of fuzzification and a defuzzification similar to that for ANFIS of one output [36].

5. Results and discussion

5.1. Prediction of distribution of heavy metals using ANN model

In this section, 73% of the datasets were assigned for training purposes, while 27% was used for testing the network performance(see Tables 3 and 4). The performance of an ANN is related to the architecture of layers and the number of neurons, which is the pattern of the connections between the neurons [32]. In order to obtain the best performance of the ANN model, it is necessary to define the optimal network architecture. Part of the sensitivity analysis of this model is shown in Table 3 and Table 4. The optimal network for this study is a feed forward multilayer perceptron having one input layer with three inputs (SO₄, Cl and TDS) and one hidden layer with seven neurons, and is fully connected to all inputs, and utilizes hyperbolic tangent sigmoid activation function (tansig). The output layer has four neurons (Fe, Mn, Pb, and Zn) with a sigmoid hyperbolic logarithm activation function (logsig). Figure 4 shows the neural network architecture.

Table 3. Part of the sensitivity analysis of ANN model for training data.

Zn		Pb		Mn		Fe		Activation functions	Model architecture
MSE	R ²								
0.69	0.02	0.08	0.53	0.04	0.25	0.05	0.44	TanSig-TanSig-TanSig	3-5-3-4
0.13	0.16	0.05	0.50	0.03	0.46	0.06	0.43	LogSig-LogSig-LogSig	3-3-3-4
0.06	0.32	0.06	0.40	0.03	0.47	0.05	0.42	Purelin-Purelin-Purelin	3-7-8-4
0.04	0.58	0.05	0.59	0.03	0.54	0.04	0.57	LogSig-LogSig-LogSig	3-8-13-4
0.05	0.51	0.06	0.47	0.04	0.49	0.06	0.45	TanSig-LogSig	3-6-4
0.04	0.58	0.06	0.54	0.02	0.69	0.03	0.70	TanSig-TanSig	3-7-4
0.02	0.79	0.02	0.79	0.01	0.72	0.03	0.71	TanSig-LogSig	3-7-4

Table 4. Part of the sensitivity analysis of ANN model for testing data.

Zn		Pb		Mn		Fe		Activation functions	Model architecture
MSE	R ²								
0.5636	0.02	0.18	0.53	0.25	0.10	0.02	0.21	TanSig-TanSig-TanSig	3-5-3-4
0.30	0.06	0.15	0.72	0.19	0.04	0.01	0.22	LogSig-LogSig-LogSig	3-3-3-4
0.15	0.17	0.04	0.31	0.16	0.15	0.04	0.52	Purelin-Purelin-Purelin	3-7-8-4
0.24	0.01	0.04	0.65	0.17	0.50	0.01	0.15	LogSig-LogSig-LogSig	3-8-13-4
0.14	0.49	0.28	0.12	0.12	0.47	0.25	0.34	TanSig-LogSig	3-6-4
0.13	0.48	0.12	0.63	0.11	0.51	0.02	0.43	TanSig-TanSig	3-7-4
0.08	0.52	0.02	0.68	0.07	0.59	0.01	0.54	TanSig-LogSig	3-7-4

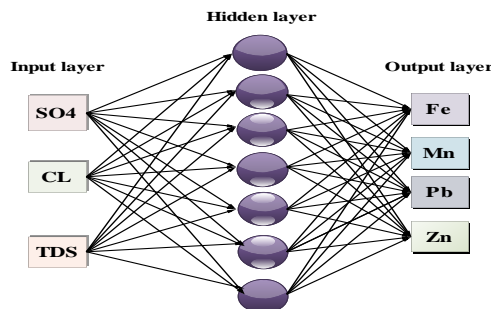


Figure 4. A neural network architecture.

5.2. Prediction of distribution of heavy metals using hybrid ANN with BBO

In this section, we used BBO to better regulate the weights and biases of the ANN model (in the previous section). Part of the sensitivity analysis of this model is shown in Tables 5 and 6. The optimal network for this study having one input layer with three inputs (SO₄, Cl, and TDS), one

hidden layer with twelve neurons, and sigmoid hyperbolic tangent (tansig) activation function. The output layer has four neurons (Fe, Mn, Pb, and Zn) with a sigmoid hyperbolic logarithm (logsig) activation function. Figure 5 shows the architecture of the ANN-BBO model. Also the control parameters used for running BBO is shown in Table 7.

Table 5. Part of the sensitivity analysis of the ANN-BBO model for training data.

Zn		Pb		Mn		Fe		Activation functions	Model architecture
MSE	R ²								
0.11	0.37	0.05	0.85	0.03	0.53	0.08	0.32	TanSig-TanSig-TanSig	3-5-3-4
0.04	0.54	0.07	0.60	0.03	0.61	0.04	0.54	LogSig-LogSig-LogSig	3-5-8-4
0.03	0.72	0.03	0.69	0.03	0.62	0.04	0.67	TanSig-LogSig	3-10-4
0.02	0.85	0.11	0.44	0.05	0.53	0.04	0.65	TanSig-LogSig	3-5-4
0.03	0.76	0.05	0.65	0.03	0.73	0.04	0.64	LogSig-LogSig	3-7-4
0.04	0.66	0.05	0.75	0.02	0.71	0.02	0.78	TanSig-LogSig	3-7-4
0.02	0.75	0.03	0.71	0.02	0.67	0.03	0.68	TanSig-LogSig	3-8-4
0.02	0.83	0.05	0.73	0.02	0.78	0.02	0.85	TanSig-LogSig	3-12-4

Table 6. Part of the sensitivity analysis of the ANN-BBO model for testing data.

Zn		Pb		Mn		Fe		Activation functions	Model architecture
MSE	R ²								
0.71	0.45	0.18	0.58	0.44	0.56	0.01	0.41	TanSig-TanSig-TanSig	3-5-3-4
0.14	0.22	0.08	0.62	0.13	0.54	0.07	0.67	LogSig-LogSig-LogSig	3-5-8-4
0.08	0.58	0.03	0.45	0.46	0.86	0.01	0.66	TanSig-LogSig	3-10-4
0.05	0.77	0.14	0.48	0.08	0.59	0.01	0.67	TanSig-LogSig	3-5-4
0.06	0.69	0.06	0.51	0.10	0.54	0.01	0.68	LogSig-LogSig	3-7-4
0.07	0.68	0.19	0.77	0.08	0.69	0.01	0.66	TanSig-LogSig	3-7-4
0.07	0.61	0.07	0.75	0.13	0.78	0.01	0.68	TanSig-LogSig	3-8-4
0.06	0.70	0.13	0.79	0.05	0.78	0.01	0.69	TanSig-LogSig	3-12-4

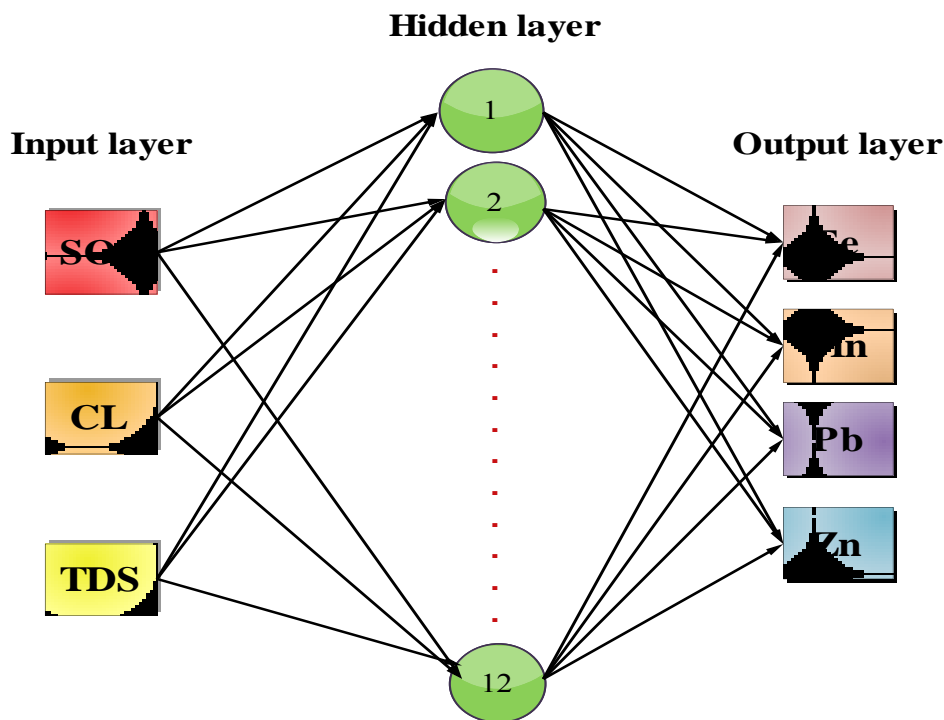


Figure 5. Architecture of e ANN-BBO model.

Table 7. Control parameters used for running BBO.

Definition	Value
Number of habitats (population size)	900
Highest number of repeat algorithm steps	200
Migration formula coefficient	0.9
Percentage of mutation	0.1
Percentage of old population that is directly transferred to the new population	0.2

5.3. Prediction of distribution of heavy metals using MANFIS-SCM model

In this study, the MANFIS-SCM model was also applied for predicting Fe, Mn, Pb, and Zn. Similar to the ANN analyses part, all the datasets were distributed randomly to the training (73%) and testing (27%) datasets.

Table 8 shows the characterizations of the MANFIS-SCM model. The optimal parameters of the MANFIS-SCM model are also shown in Table 9. Part of the sensitivity analysis of this model is shown in Tables 10 and 11.

Table 8. Characterizations of MANFIS-SCM model.

ANFIS parameter	Value
Number of training data pairs	38
Number of testing data pairs	14
Input membership function	Gaussianmf
Output membership function	Linear
Number of nodes	38
Number of linear parameters	16
Number of non-linear parameters	24
Total number of parameters	40
Number of fuzzy rules	4

Table 9. Optimal parameters of MANFIS-SCM model.

Parameter	Value
Number of periodic training Process	100
Error goal	0
Initial step size	0.01
Step size decrease rate	0.5
Step size increase rate	0.9

Table 10. Part of the sensitivity analysis of MANFIS-SCM model for training data.

Zn		Pb		Mn		Fe		Number of periodic training process	Influence radius
MSE	R ²								
0.09	0.85	0.01	0.77	0.01	0.95	0.01	0.71	1000	1
0.01	0.99	0.01	0.99	0.01	0.99	0.01	0.99	50	0.3
0.01	0.99	0.01	0.99	0.01	0.99	0.01	0.99	500	0.25
0.01	0.99	0.01	0.99	0.01	0.99	0.01	0.99	1000	0.4
0.01	0.98	0.01	0.88	0.01	0.93	0.01	0.98	500	0.82
0.01	0.99	0.01	0.97	0.01	0.93	0.01	0.98	100	0.75
0.01	0.99	0.01	0.98	0.01	0.98	0.01	0.99	100	0.65

Table 11. Part of the sensitivity analysis of ANFIS model for testing data.

Zn		Pb		Mn		Fe		Number of periodic training process	Influence radius
MSE	R ²								
0.24	0.89	0.01	0.14	0.03	0.77	0.01	0.44	1000	1
4.93	0.37	0.08	0.32	0.05	0.64	0.03	0.21	50	0.3
6.43	0.48	0.08	0.29	0.41	0.91	0.04	0.46	500	0.25
0.91	0.68	0.09	0.06	0.05	0.75	0.10	0.58	1000	0.4
1.05	0.60	0.01	0.09	0.03	0.82	0.01	0.38	500	0.82
0.75	0.765	0.01	0.74	0.02	0.84	0.02	0.61	100	0.75
0.69	0.78	0.01	0.85	0.01	0.92	0.05	0.60	100	0.65

Table 12. A comparison between the results of intelligent models used for training data.

Modeling approach	Outputs	MSE	R ²
MANFIS-SCM model	Fe	0.01	0.99
	Mn	0.01	0.98
	Pb	0.01	0.98
	Zn	0.01	0.99
ANN-BBO model	Fe	0.02	0.85
	Mn	0.02	0.78
	Pb	0.05	0.73
	Zn	0.02	0.83
ANN model	Fe	0.03	0.71
	Mn	0.01	0.72
	Pb	0.02	0.79
	Zn	0.02	0.79

Table 13. A comparison between the results of intelligent models used for testing data.

Modeling approach	Outputs	MSE	R ²
MANFIS-SCM model	Fe	0.05	0.60
	Mn	0.01	0.92
	Pb	0.01	0.84
	Zn	0.69	0.78
ANN-BBO model	Fe	0.01	0.69
	Mn	0.05	0.78
	Pb	0.12	0.79
	Zn	0.06	0.70
ANN model	Fe	0.01	0.54
	Mn	0.07	0.59
	Pb	0.02	0.68
	Zn	0.08	0.52

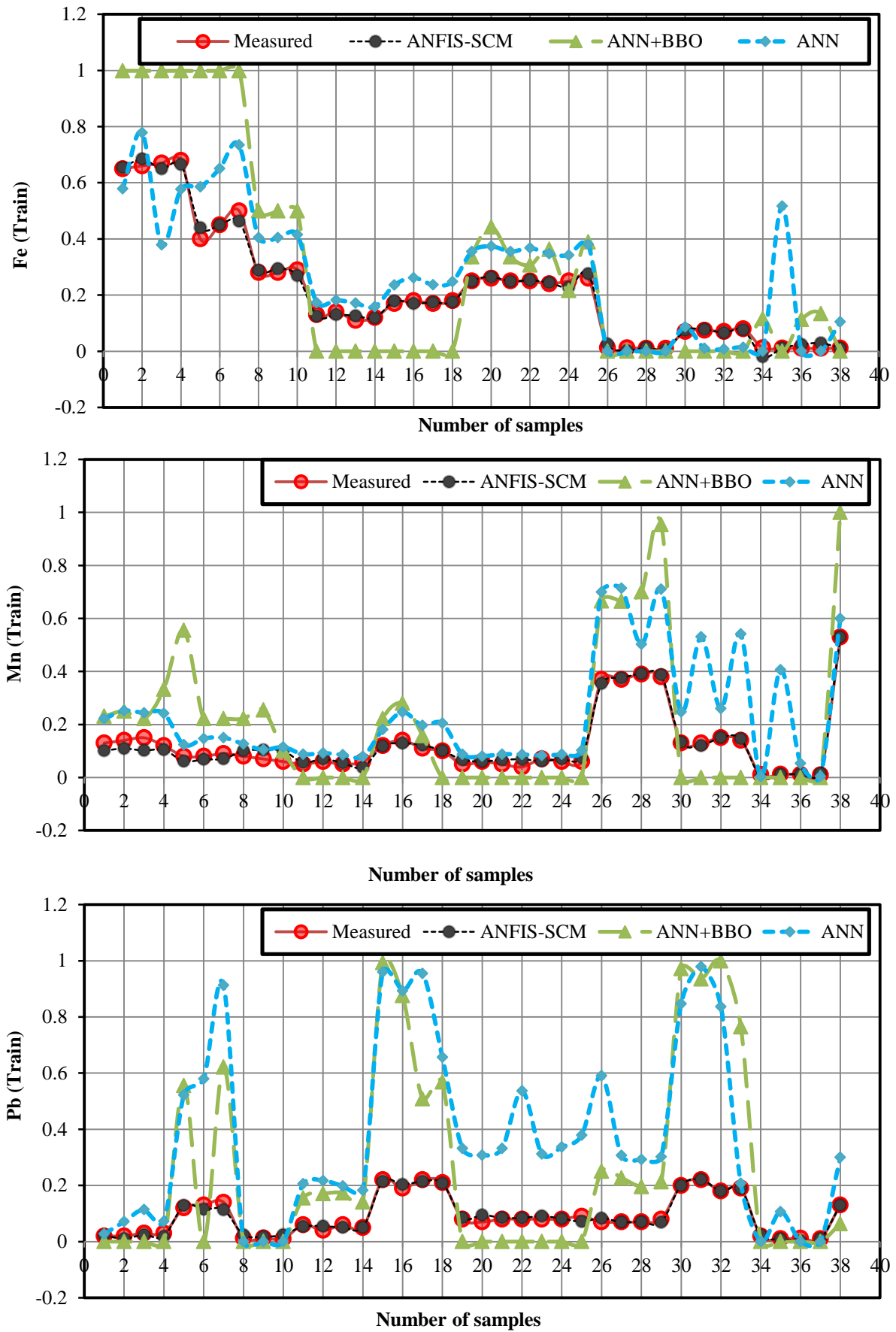


Figure 6. A comparison between the predicted values for metals by the ANN, ANN-BBO, and MANFIS-SCM models and measured values for training datasets.

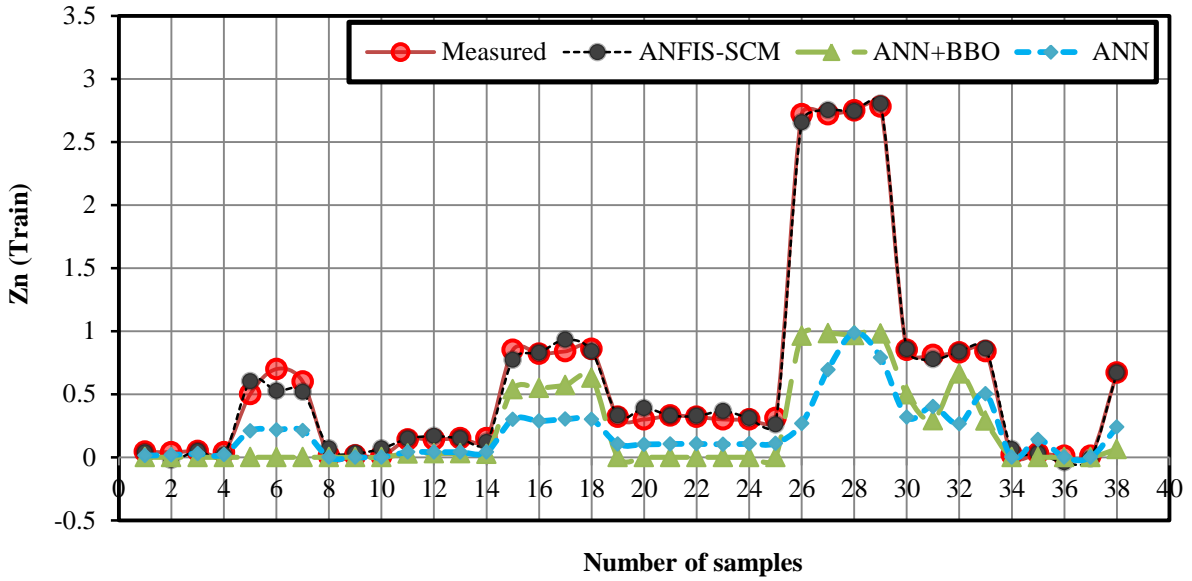


Figure 6. Continued.

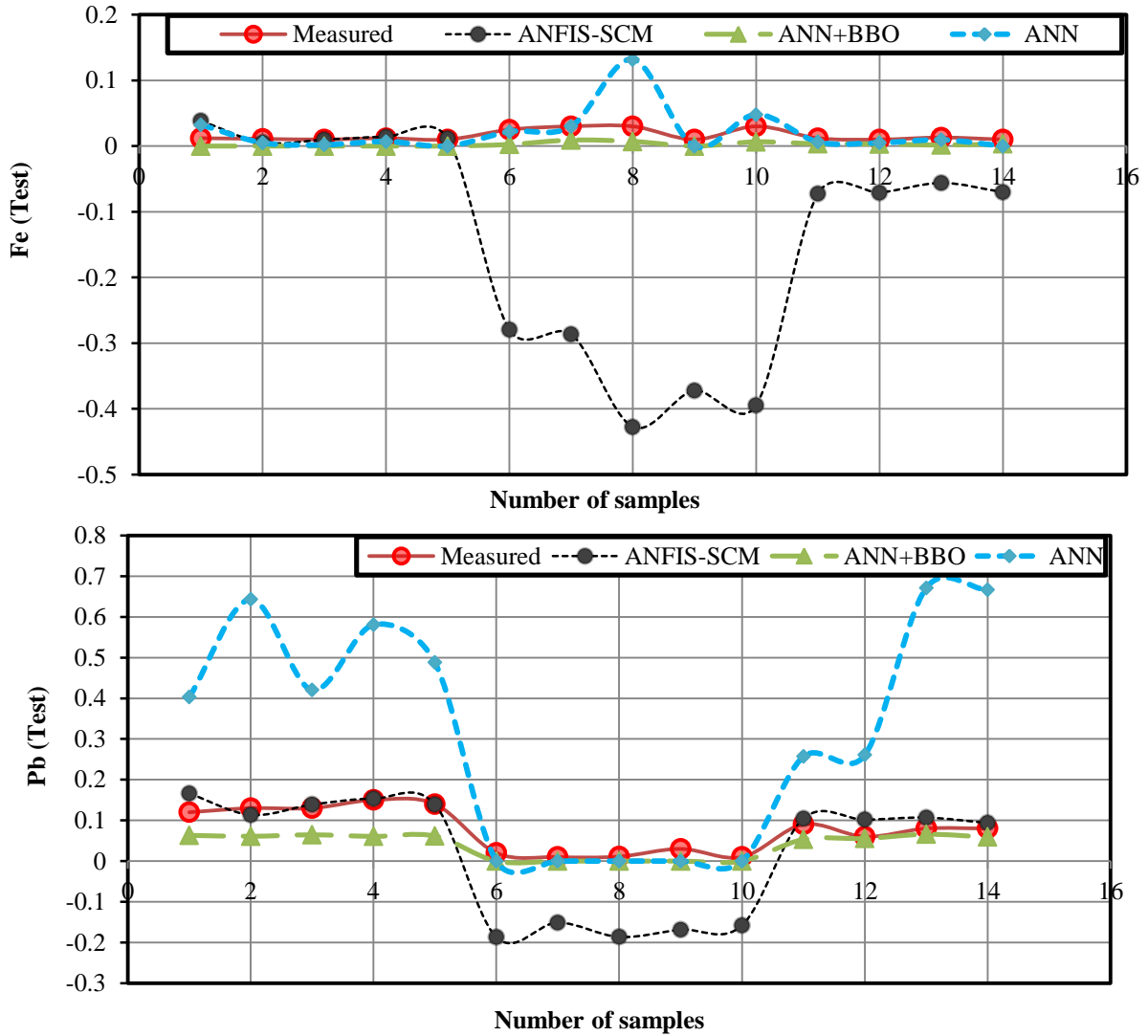


Figure 7. A comparison between the predicted values for metals by ANN, ANN-BBO, and MANFIS-SCM models and measured values for testing datasets.

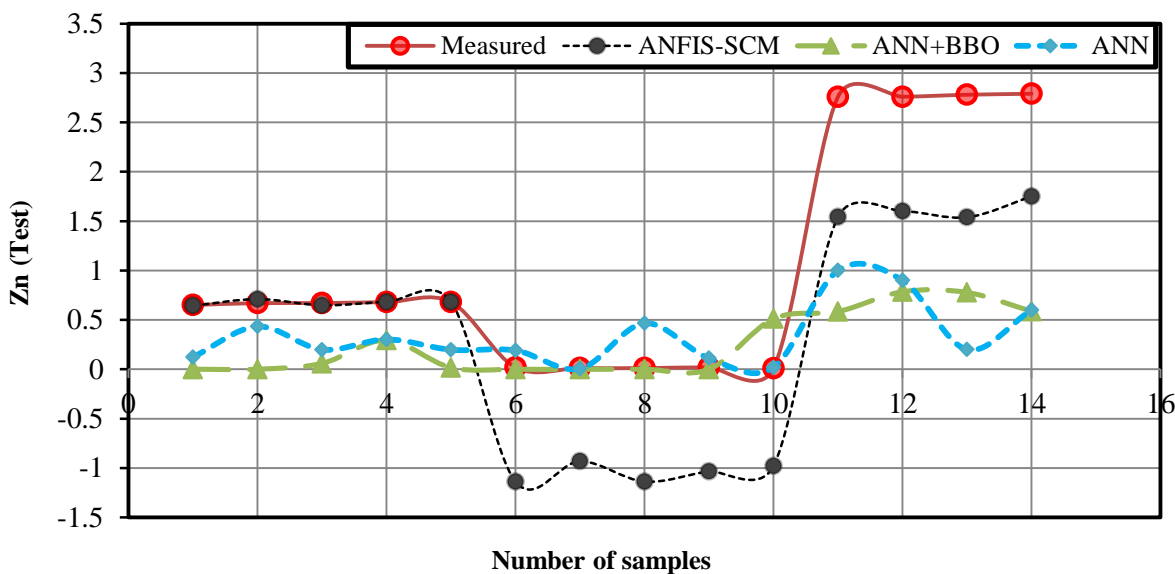
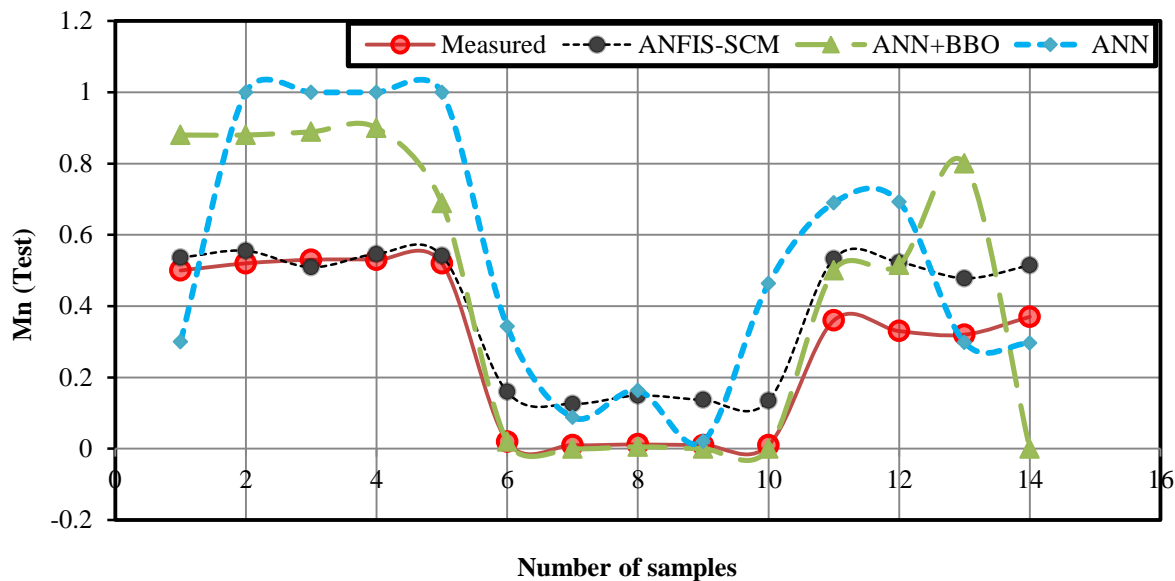


Figure 7. Continued.

6. Conclusions

High concentrations of Fe, Mn, Pb, and Zn were found in the groundwater of the Lakan lead-zinc minedue to impacts from historical mining operations. In this paper, theANN, ANN-BBO, and MANFIS-SCM modelswere developed to estimate the heavy metals concentrations in groundwater using SO₄, Cl, and TDS as input parameters, and Fe, Mn, Pb, and Zn as output parameters, and the following remarks were concluded:

- Implementation hybrid for BBO as an optimizer of connection weights of ANN to predict the heavy metal concentrations in groundwater was demonstrated in detail.
- It was determined that the MANFIS-SCM model was a reliable technique for estimating

heavy metals in groundwater with an acceptable degree of accuracy and robustness.

Acknowledgments

The chemical analyses were conducted at the laboratory of the Department of Mining Engineering, Arak University of Technology. The authors wish to thank Arak University of Technology for their continuous support.

References

[1]. Moncur, M.C., Ptacek, C.J, Blowes, D.W. and Jambor, J.L. (2005). Release, transport and attenuation of metals from an old tailings impoundment. Appl Geochem. 20: 639-659.
 [2].Rogers, L.L. and Dowla, F.U. (1994). Optimization Of groundwater mediation using artificial neural

networks with parallel solute transport modeling, *Water Res. Res.* 30 (2): 457-481.

[3].Schleiter, L.M., Borchardt, D., Wagner, R.T., Dapper, T., Schmidt, K.D. and Schmidt, H.H. (1999). Modelling water quality, bioindication and population dynamics in lotic ecosystems using neural networks. *Ecological Modelling*. 120: 271-286.

[4].Gizogluj, H.K. (2002). Suspended Sediment Estimation for Rivers using Artificial Neural Networks and Sediment Rating Curves. *Turkish J.Eng Env Sci.* 26: 27-36.

[5].Kemper, T. and Sommer, S. (2002). Estimate of heavy metal contamination in soils after a mining accident using reflectance spectroscopy. *Environ Sci Technol.* 36: 2742-2747.

[6].Liu, C.W., Kuo, Y.M. and Lin, K.H. (2004). Evaluation of the ability of an artificial neural network model to assess the variation of groundwater quality in an area of blackfoot disease in Taiwan. *Water Research*. 38: 148-158.

[7].Almasri, M.N. and Kaluarach, J.J. (2005). Modular neural networks to predict the nitrate distribution in ground water using the on-ground nitrogen loading and recharge data. *Environmental Modelling & Software*. 20:851-871.

[8]. Palani, S., Liong, S.Y. and Tkalich, P. (2008). An ANN application for water quality forecasting. *Marine Pollution Bulletin*. 56: 1586-1597.

[9]. Noori, R., Khakpour, A., Omidvar, B. and Farokhnia, A. (2010). Comparison of ANN and principal component analysis-multivariate linear regression models for predicting the river flow based on developed discrepancy ratio statistic. *Expert Systems with Applications*. 37: 5856-5862.

[10]. Rooki, R., Doulati Ardejani, F., Aryafar, A. and Bani Asadi, A. (2011). Prediction of heavy metals in acid mine drainage using artificial neural network from the Shur River of the Sarcheshmeh porphyry copper mine, Southeast Iran. *Environ Earth Sci*: DOI 10.1007/s12665-011-0948-5.

[11]. Heydar, M., Olyaie, E., Mohebzadeh, H. and Kisi, O. (2013). Development of a Neural Network Technique for Prediction of Water Quality Parameters in the Delaware River, Pennsylvania. *Middle-East Journal of Scientific Research*. 13 (10): 1367-1376.

[12]. Badaoui, H.E., Abdallaoui, A., Manssouri, I. and Lancelot, L. (2013). Application of the Artificial Neural Networks of MLP Type for the Prediction of the Levels of Heavy Metals in Moroccan Aquatic Sediments. *International Journal of Computational Engineering Research*. 3 (6):75-81.

[13].Irfan Yesilnacar, M. and Sahinkaya, E. (2012). Artificial neural network prediction of sulfate and SAR in an unconfined aquifer in southeastern

Turkey, *Environmental Earth Sciences*. 67(4): 1111-1119.

[14]. Keskin, T., Düğenci, M. and Fikrt Kaçaroğlu, F. (2015). Prediction of water pollution sources using artificial neural networks in the study areas of Sivas, Karabük and Bartın (Turkey). *Environmental Earth Sciences*. 73 (9) 5333-5347.

[15].Nasr, M. and Zahran, H.F. (2014). Using of pH as a tool to predict salinity of groundwater for irrigation purpose using artificial neural network. *Egyptian Journal of Aquatic Research*. 49 (2): 111-115.

[16]. Grande, J.A., Andujar, J.M., Aroba, J. and Torre, M.L. (2009). Presence of As in the fluvial network due to AMD processes in the Riotinto mining area (SW Spain): A fuzzy logic qualitative model. *Journal of Hazardous Materials*. 176: 395-401.

[17]. Yan Zou, H.Z. and Wang. H. (2010). Adaptive neuro fuzzy inference system for classification of water quality status. *Journal of Environmental Sciences*. 22 (12): 1891-1896.

[18]. Sahu, H.B., Padhee, S. and Mahapatra, S.S. (2010). Prediction of spontaneous heating susceptibility of Indian coals using fuzzy logic and artificial neural network models. *Expert Systems with Applications*. 38: 2271-2282.

[19]. Valente, T., Ferreira, M.J., Grande, J.A., Torre, M.L.D.L. and Borrego, J. (2013). PH, electric conductivity and sulfate as base parameters to estimate the concentration of metals in AMD using a fuzzy inference system. *Journal of Geochemical Exploration*. 124: 22-28.

[20]. Mohammadi, L. and Meech, J.A. (2012). AFRA - Heuristic expert system to assess the atmospheric risk of sulphide waste dumps. *Journal of Loss Prevention in the Process Industries*. 26: 261-271.

[21]. Zhang, H., Song, J., Su, C. and He, M. (2012). Human attitudes in environmental management: Fuzzy Cognitive Maps and policy option simulations analysis for a coal-mine ecosystem in China. *Journal of Environmental Management*. 115: 227-234.

[22]. Liu, D. and Zou, Z. (2012). Water quality evaluation based on improved fuzzy matter-element method. *Journal of Environmental Sciences*. 24 (7): 1210-1216.

[23].Pourjabbar, A., Sârbu, C., Kostarelos, K., Einax, J.W. and Büchel, G. (2014). Fuzzy hierarchical cross-clustering of data from abandoned mine site contaminated with heavy metals. *Computers & Geosciences*. 72: 122-133.

[24]. Mahdevari, S., Shahriar, K. and Esfahanipour, A. (2014). Human health and safety risks management in underground coal mines using fuzzy TOPSIS. *Science of the Total Environment*. 488-489: 85-99.

- [25]. Chang, F.J., Chung, C.H., Chen, P.A., Liu, C.W., Coynel, A. and Vachaud, G. (2014). Assessment of arsenic concentration in stream water using neuro fuzzy networks with factor analysis. *Science of the Total Environment*. 494-495: 202-210.
- [26]. Maiti, S. and Tiwari, R. K. (2014). A comparative study of artificial neural networks, Bayesian neural networks and adaptive neuro-fuzzy inference system in groundwater level prediction. *Environmental Earth Sciences*. 71 (7): 3147-3160.
- [27]. Ghadimi, F. (2015). Prediction of heavy metals contamination in the groundwater of Arak region using artificial neural network and multiple linear regression. *Journal of Tethys*. 3 (3): 203-215.
- [28]. GSI. (2007). Geological map of Varcheh Khomain. Geological Society of Iran.
- [29]. Ghadimi, F., Ghomi, M. and Hajati, A. (2012). Identification of groundwater contamination sources of Lakan lead and zinc mine, Khomain, Iran., *Journal of Mining and Environment*. 3 (2): 121-134.
- [30]. Jorjani, E., Chehreh Chelgani, S. and Mesroghli, S.H. (2008). Application of artificial neural networks to predict chemical desulfurization of Tabas coal. *Fuel*. 87: 2727-2734.
- [31]. Yao, H.M., Vuthaluru, H.B. and Tade, M.O. (2005). Djukanovic D. Artificial neural networkbased prediction of hydrogen content of coal in power station boilers. *Fuel*. 84: 1535-42.
- [32]. Hajihassani, M., Jahed Armaghani, D., Sohaei, H., Tonnizam Mohamad, E. and Marto, A. (2014). Prediction of airblast-overpressure induced by blasting using a hybrid artificial neural network and particle swarm optimization. *Appl Acoust*. 80: 57-67.
- [33]. Simon, D. (2008). Biogeography-based Optimization. *IEEE Trans. Evol. Comput*. 12 (6): 702-713.
- [34]. Zadeh, L.A. (1965). Fuzzy sets. *Inform Control*. 8: 338-353.
- [35]. Takagi, T. and Sugeno, M. (1985). Fuzzy identification of systems and its applications to modeling and control. *IEEE Trans Syst Man Cybernet*. 15: 116-32.
- [36]. Wesley, J. (1997). *Fuzzy and Neural Approaches in Engineering*. Hines New York.

کاربرد روش‌های هوش مصنوعی در پیش‌بینی توزیع عناصر سنگین در آب زیرزمینی معدن سرب و روی لکان، ایران

زهره بیات زاده فرد، فریدون قدیمی* و هادی فتاحی

دانشکده مهندسی معدن، دانشگاه صنعتی اراک، اراک، ایران

ارسال ۲۰۱۶/۱/۱۰، پذیرش ۲۰۱۶/۲/۲۲

* نویسنده مسئول مکاتبات: ghadimi@arakut.ac.ir

چکیده:

تعیین توزیع عناصر سنگین در آب زیرزمینی از مسائل با اهمیت در حوزه مدیریت و فعالیت‌های معدنکاری است. در این تحقیق با استفاده از روش‌های هوش مصنوعی از جمله: شبکه عصبی مصنوعی، ترکیب شبکه عصبی مصنوعی- الگوریتم بهینه‌سازی جغرافیای زیستی و سیستم استنتاج تطبیقی نرو- فازی چند خروجی برای پیش‌بینی تعیین توزیع عناصر سنگین در آب زیرزمینی در منطقه معدنی لکان خمین مورد استفاده قرار گرفت. به همین منظور منابع آلودگی آب زیرزمینی با استفاده از داده‌های کمی موجود و چندین مدل هوش مصنوعی جهت مدل‌سازی (با سه ورودی و چهار خروجی) مورد آموزش و تست مورد تحلیل قرار گرفت. از بین مدل‌ها، روش سیستم استنتاج تطبیقی نرو- فازی چند خروجی به عنوان بهترین مدل انتخاب شد. نتایج نشان می‌دهد که این مدل برای پیش‌بینی تعیین توزیع عناصر سنگین در آب زیرزمینی از قابلیت بالایی برخوردار است.

کلمات کلیدی: آب زیرزمینی، شبکه عصبی مصنوعی، سیستم استنتاج تطبیقی نرو- فازی چند خروجی، عناصر سنگین، الگوریتم بهینه‌سازی جغرافیای زیستی.